Journal of Photochemistry and Photobiology A: Chemistry 217 (2011) 157–163

Contents lists available at ScienceDirect

Journal of Photochemistry and Photobiology A: Chemistry

journal homepage: www.elsevier.com/locate/jphotochem

Photochemical behavior in azobenzene having acidic groups. Preparation of magnetic photoresponsive gels

Gonzalo Abellán[a], Hermenegildo García[b,*], Carlos J. Gómez-García[a], Antonio Ribera[a,c,**]

[a] Instituto de Ciencia Molecular, Universidad de Valencia, Catedrático José Beltrán 2, 46980, Paterna, Valencia, Spain
[b] Instituto de Tecnología Química CSIC-UPV, Universidad Politécnica de Valencia, Avenida de los Naranjos s/n, 46022 Valencia, Spain
[c] Fundación General de la Universidad de Valencia (FGUV), Amadeu de Savoia n° 4, 46010 Valencia, Spain

ARTICLE INFO

Article history:
Received 22 July 2010
Received in revised form
30 September 2010
Accepted 2 October 2010
Available online 28 October 2010

Keywords:
Photoisomerization
Azobenzene
Laser flash photolysis
Photoresponsive gel
Magnetite nanoparticles
Multifunctional materials

ABSTRACT

The photochemistry of three azobenzenes representing contrasting photochemical behaviors is described in the present work. Thus, Methyl Orange (MO, 4-[[(4-dimethylamino)phenyl]-azo]benzenesulfonic acid sodium salt, hereinafter (**1**) and 4-hydroxyazobenzene-4′-sulfonic acid (**2**) undergo in water fast photochemical proton shift, with decays in the microsecond timescale. In contrast to the previous cases, azobenzene-4,4′-dicarboxylic acid (**3**) undergoes photoisomerization in water. This photochemical behavior allows the preparation of aqueous gels with Aerosil as gelating agent (5% weight) exhibiting high cyclability and photoreversible isomerization of the *trans* to *cis* (300 nm irradiation) and *cis* to *trans* (visible white light irradiation). Gels containing azobenzene **3** as photoresponsive molecule and well-dispersed magnetite (Fe_3O_4) nanoparticles exhibit simultaneously high photoresponse and magnetic properties. Photoisomerization of compound **3** in these gels leads to small but reliable changes (25 G coercive field) in the magnetic hysteresis loop of magnetite nanoparticles. This novel concept of optical modulation of magnetism in iron oxide nanoparticles paves the way for the study of new systems, with a stronger coupling between *trans–cis* photoisomerization and magnetic properties.

1. Introduction

Photochemical isomerization of *trans* azobenzenes to the *cis* isomers and the corresponding dark (thermal), or photochemical relaxation to the most stable *trans* isomer of the azocompound has attracted a considerable attention from the fundamental [1–4] and applied points of view [5–14]. In general this photoisomerization can be conveniently followed by monitoring the optical spectrum since *trans* isomers absorb at around 350 nm, while the *cis* isomers typically exhibit a less intense absorption band at longer (around 450 nm) wavelengths [1,3]. The significant variation of the absorption band from *trans* to *cis* is useful, not only to follow the photoisomerization, but also to induce specifically the transformation of the *trans* into the *cis* (with UV light) and the conversion of the *cis* into the *trans* (with visible light), that can be employed to control at will the configuration of the molecule [1].

One of the most notable consequences of the *trans* to *cis* isomerization is the dramatic change of molecule's length, that for the parent azobenzene changes from 9.0 Å for the *trans* isomer to 5.5 Å of the *cis* azobenzene isomer, this change in the molecular dimensions is among the largest possible for a reversible reaction [2].

Since the establishment of methods to control the narrow size distribution of nanoparticles [15], materials including metal and metal-oxide nanoparticles in combination with organic molecules and/or polymers have been widely reported [16], searching for new and enhanced properties relative to their individual components, based on the interaction between the metal or metal-oxide nanoparticles and the organic molecules and/or polymers [17]. Unfortunately, an important part of these materials are based on organic matrix that fall in a low chemical durability and mechanical resistance.

Recently, sol–gel derived inorganic matrices have been used as hosts due to their good chemical and mechanical stability and moreover, the synthesis is performed at low temperature, which is appropriated for the thermal stability of organic molecules [18].

The aim of this study is to present data of photoisomerization of three 4,4′-azobenzenes having acid groups as substituent (see Scheme 1), showing the behavior in water and in a silica gel matrix. Our study is complemented with laser flash photolysis data and analysis of the photoreaction process to rationalize the results pre-

* Corresponding author. Tel.: +34 62095 2690; fax: +34 96387 7809.
** Corresponding author at: Instituto de Ciencia Molecular, Universidad de Valencia, Catedrático José Beltrán 2, 46980, Paterna, Valencia, Spain.
Tel.: +34 96354 4419; fax: +34 96354 3273.
E-mail addresses: hgarcia@qim.upv.es (H. García), antonio.ribera@uv.es (A. Ribera).
URLs: http://www.upv.es/itq (H. García), http://www.icmol.es (A. Ribera).

1010-6030/$ – see front matter © 2010 Elsevier B.V. All rights reserved.
doi:10.1016/j.jphotochem.2010.10.003

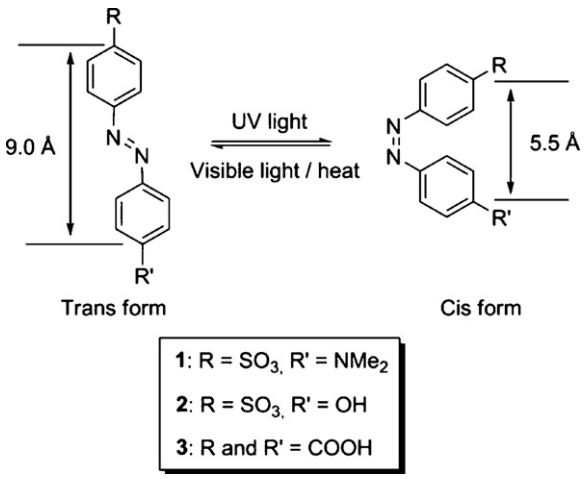

Scheme 1. Variation in the molecular dimensions upon *cis–trans* isomerization and structure of the three azocompounds under study.

sented. The three azobenzenes under study have in common the possession of acids groups, whose presence would make possible to complete the *trans*/*cis* isomerization with the use of these molecules as ligand of magnetite nanoparticles. The novel concept of our work is to couple the well-studied reversible *cis*/*trans* isomerization of azobenzenes with the magnetic properties of iron oxide nanoparticles. The presence of acids groups as substituents of azobenzenes would allow coordination of these photoresponsive molecules with the nanoparticles. In the long-term we are interested in developing systems in which azobenzene photoisomerization can switch in a controllable manner the magnetic properties of metal oxides. Towards this goal, herein we have prepared gels that have been magnetically characterized before and after UV irradiation showing, indeed, that the photoisomerization modifies the hysteresis loop when azobenzenes with acid groups are coordinated to the nanoparticles.

2. Results and discussion

Preliminary studies with the three azobenzenes in aqueous solutions (about 10^{-5} M) were carried out under steady state irradiation. Although some minor changes were observed in the 210–240 nm region for **1**, this azocompound basically does not undergo any change in the optical spectrum under these conditions (Fig. 1). Considering the short wavelength in which the changes are observed (<250 nm) these small variations could be due to some impurities formed in small amounts during the photochemical treatment and unrelated to the *cis*/*trans* isomerization.

In the case of 4-hydroxy, 4′-sulfonic substituted azocompound **2**, irradiation at 355 nm with quasi monochromatic mercury lamps in water (pH 6.3) leads to relatively minor changes in the 300–520 nm region that are compatible with the occurrence of some photoisomerization to reach a photostationary *trans*/*cis* mixture different from the initial state. In addition also some minor variations in the 200–240 nm region were also observed (Fig. 2). As commented in the case of compound **1**, variations of the absorbance in such short wavelength region, are most likely due to the formation of impurities, even in trace amounts, during the photochemical irradiation.

More interesting from the point of view of the photochemical isomerization under amenable conditions was the behavior of symmetric 4,4′-dicarboxylate azobenzene **3**. In this case it has to be noted that the pH of the aqueous solution was set to 11 to facilitate the solubility of the azobenzene **3** [19]. As it can be seen in Fig. 3, 355 nm steady state irradiation of compound **3** leads to a

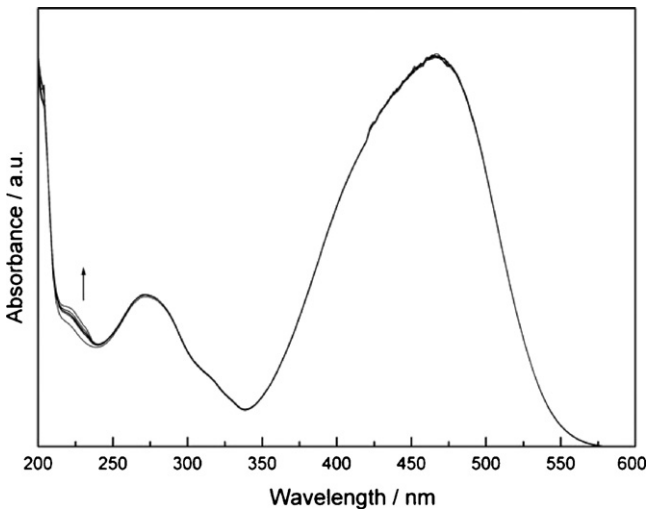

Fig. 1. Absorption spectra of **1** under UV irradiation in water. The arrows indicate the growth or decrease of the absorption band upon UV irradiation.

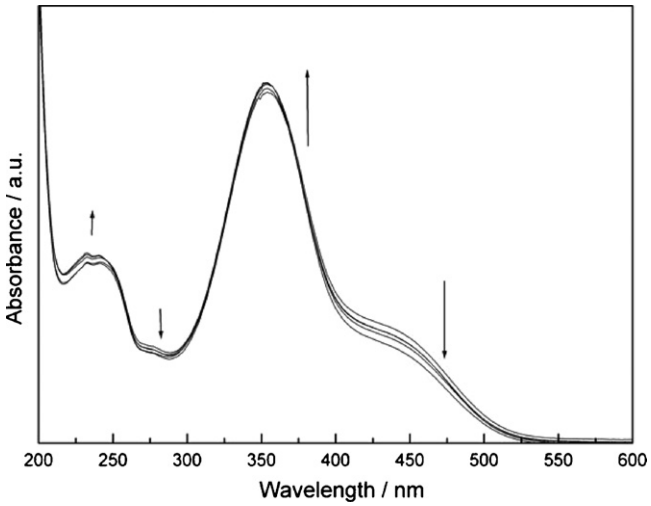

Fig. 2. Absorption spectra of **2** under UV irradiation in water, showing some minor variations in the 200–240 nm region upon UV irradiation.

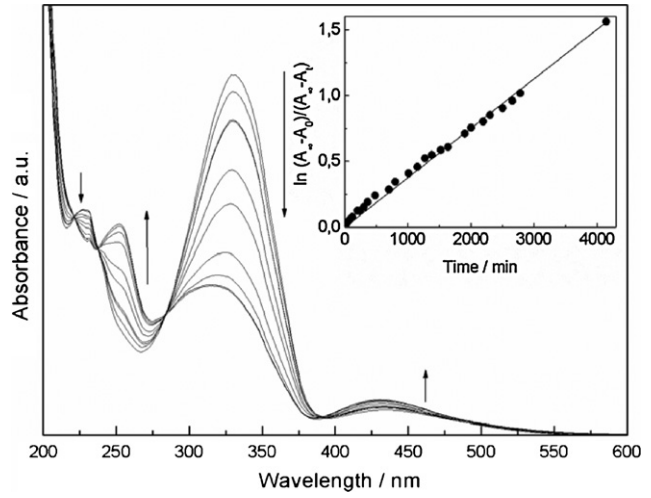

Fig. 3. Absorption spectra of **3** under UV irradiation in water. The peaks at about 330 nm are characteristic of the *trans* isomer, while the peaks at about 430 nm correspond to the *cis* isomer. The series of spectra presented correspond to the visible light photoisomerization of the *cis* isomer into the *trans*. The inset shows a first order plot for *cis* to *trans* thermal isomerization.

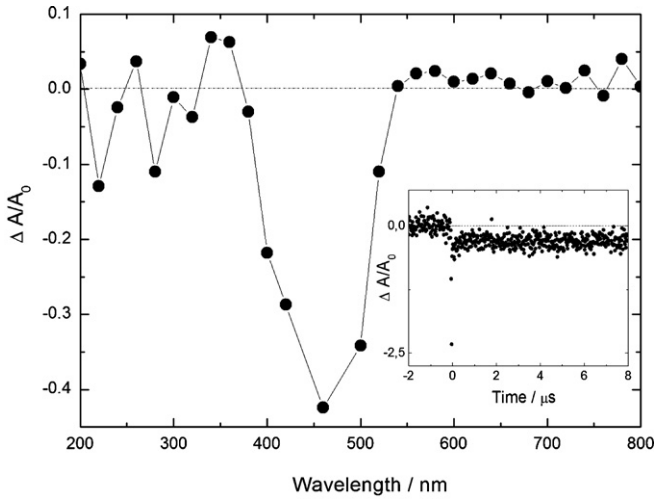

Fig. 4. Transient UV–visible absorption spectra given as variation of absorbance, ΔA, divided by the initial absorption of an O_2-purged **1** solution recorded 1 μs after 355 nm laser excitation. The inset shows the temporal signal decay measured at 460 nm.

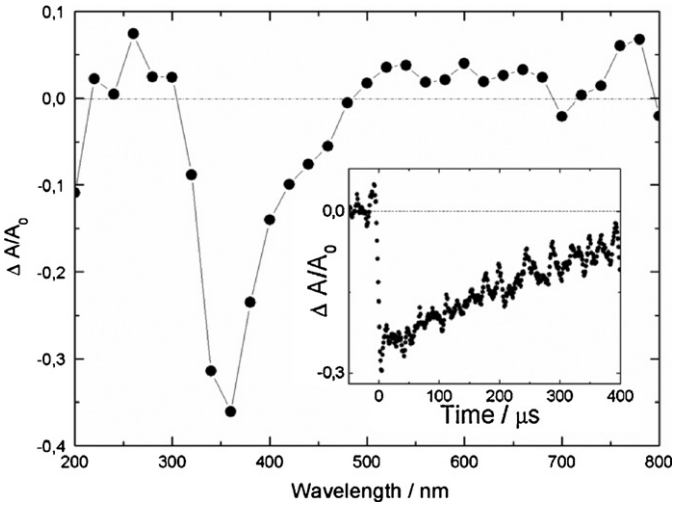

Fig. 5. Transient UV–visible absorption spectra given as variation of absorbance, ΔA, divided by the initial absorption of an O_2-purged **2** solution recorded 250 μs after 355 nm laser excitation. The inset shows the temporal signal decay measured at 360 nm.

gradual decrease of the 330 nm band and 228 nm corresponding to the *trans* isomer accompanied by a concomitant increase of the 430 nm and 250 nm bands of the *cis* isomer. Observation of four isosbestic points at 226, 238, 284 and 393 nm indicates the interconversion of the initial *trans* isomer to the *cis*. It should be noted that compounds **1** and **2** even at pH 11 exhibit exactly the same behavior (i.e. lack of evidence for *trans-cis* photoisomerization) that was observed when these compounds were irradiated at the pH that results from adding the compounds to solution. After photochemical isomerization using quasi-monochromatic UV-lamps, the course of thermal isomerization of the photogenerated *cis* isomer to the more stable *trans* isomer was followed in the dark (∼25 °C) by monitoring the band corresponding to the *trans* isomer (330 nm). Fitting of the experimental data to a first order kinetics (see inset of Fig. 3) has allowed an estimation of the value of the rate of the *cis* to *trans* thermal isomerization of 3.8×10^{-4} min^{-1}.

Since in the case of methyl orange (**1**) we have not been able to obtain any evidence of the photoisomerization using conventional spectroscopy, we have submitted an aqueous solution of **1** after 15 min purging with oxygen to laser flash photolysis using a nanosecond system and operating at 355 nm as excitation wavelength. The presence of oxygen during the experiment should suppress the formation of any triplet excited state that could mask the spectral changes of the isomerization. In principle *trans–cis* isomerization should occur independently of the presence of oxygen [20]. Under these conditions we have been able to record a transient spectrum showing an absorption band from 340 to 400 nm accompanied by an intense bleaching of the ground state absorption peaking at 455 nm and a continuous absorption from 500 to 800 nm (see Fig. 4). The temporal profile of the signals in the 500–800 broad band is identical showing that this absorption corresponds to a single species that do not correspond to the *cis* isomer. For the *cis* isomer a narrower band from 500 to 600 nm should have been recorded. Based on precedents in the literature we attribute the continuous 500–800 nm absorption to a photochemical proton shift mediated by the solvent in which, at the pH studied, a proton from the dimethyl amino substituent move to the azo group [21]. Similarly laser flash photolysis of azobenzene **2** in water was performed in the presence of oxygen to avoid the interference of the triplet excited state. Fig. 5 shows the corresponding transient spectrum recorded upon 355 nm excitation. As it can be seen there, this transient spectrum has many similarities with that previously commented from azobenzene **1**, i.e., narrow absorption peaking at 260 nm, bleaching of the *trans* isomer at 360 nm and a continuous absorption from 470 to 800 nm, and it was again attributed to photoinduced proton transfer from the phenolic to the azo group mediated by the solvent. One interesting difference between azobenzenes **1** and **2** is the lifetime of the initial *trans* isomer. This increased lifetime of the species arising from prototropism of compound **2** has to be related with the stability of the corresponding phenolate, with respect to the acid/base equilibrium corresponding to azobenzene **1**. In any case for azobenzene **1** and **2** under the conditions studied, laser flash photolysis clearly rules out the occurrence of *trans* to *cis* photoisomerization.

Compounds **1**, **2** and **3** were used to prepare gels that could exhibit photoresponse as consequence of the *trans*/*cis* isomerization. As observed in aqueous solution only compound **3** exhibits reversible photoisomerization upon UV irradiation (see SI-1, SI-2 and SI-3, respectively). In contrast to solutions, the much higher viscosity of gels allows the formation of thick films and other bulky systems containing indefinitely persistent suspended micro-/nano particles. The reduced diffusion and mobility of suspended particles occurring in gels is not possible in solution. In our case the gels were obtained by suspending Aerosil (5% weight) in water containing **3**, then the suspension was vigorous stirred and mild heated at 70 °C until thick gel was obtained. Irradiation of this gel containing **3** leads to changes in the optical spectrum, compatible with the occurrence of *trans–cis* isomerization observed for this compound in aqueous solution [22]. The two main differences of the photoisomerization in gel and in liquid phase are the extent of the decrease/increase of the bands corresponding to the *trans–cis* isomers (which is smaller in gel than in solution), and the kinetics of the reverse *cis* to *trans* isomerization that is much slower in the gel than in solution [23,24]. Consecutive cycles of *trans* to *cis* isomerization irradiating at 300 nm and *cis* to *trans* by irradiation in the visible were performed up to 10 times, without observing significant fatigue in the system. Considering that the increased viscosity of gels could favor the *trans* to *cis* isomerization of azobenzenes **1** and **2**, despite that these process do not occur in aqueous solution, we also studied the photochemical behavior of two analogous gels prepared by incorporating azobenzene **1** or **2**. However, like in solution, also for the gels we have been unable to obtain any spectroscopic evidence that could support the occurrence of *trans* to *cis*

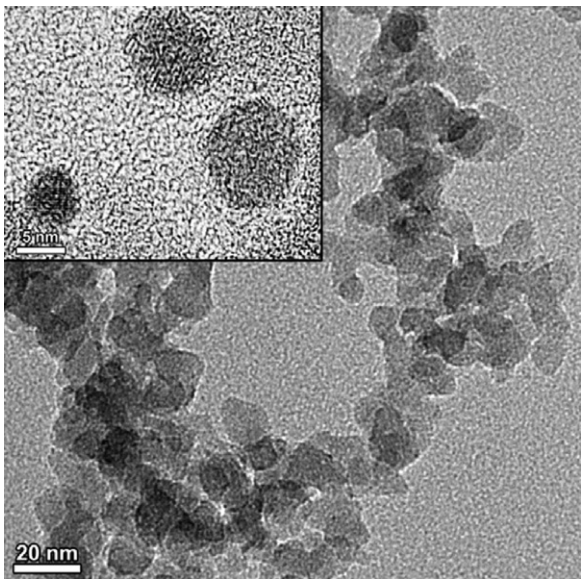

Fig. 6. HRTEM micrograph of the photoresponsive magnetic gel containing azocompound **3**. Scale bar 20 nm. The inset shows a HRTEM image of magnetite nanoparticles obtained with a higher magnification. Scale bar 5 nm.

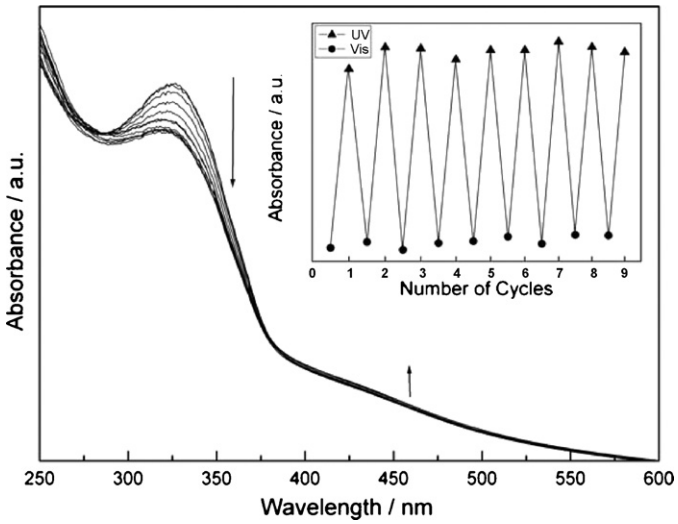

Fig. 7. Absorption UV–vis spectra of the photoresponsive gel containing iron oxide nanoparticles. The peak at about 330 nm is characteristic of the *trans* isomer, while the peak at about 430 nm corresponds to the *cis* isomer. The inset shows the reversibility data monitored at 324 nm to 327 nm after successive cycles of irradiation with UV and visible light.

photoisomerization, and therefore, no further studies with these two azobenzenes were pursued.

One advantage of gels with respect to liquid solutions is the possibility to add, together with the azocompound **3**, nanoparticles homogeneously dispersed in the medium, providing in this way, additional functionalities and properties coming from the nanoparticles [16f,25], to the already existing photoresponse provided by the *trans-cis* isomerization of the azocompound. In the present case, we have prepared a gel in which in addition to azocompound **3**, magnetite nanoparticles (average particle size 10 nm) were also incorporated. The purpose is to disclose if the photochemical *trans* to *cis* isomerization observed for azocompound **3** can lead to changes in the magnetic properties of Fe_3O_4 nanoparticles. The preparation of the material started by the synthesis of the Fe_3O_4 nanoparticles, using the high temperature decomposition of the $Fe(acac)_3$ precursor in organic phase, following the method described by Sun and Zeng [26]. This method guarantees the small size and the monodispersity of the nanoparticles. However it presents the disadvantage, from the point of view of the synthesis of the gel, of requiring organic solvent. This inconvenience was solved including an aqueous phase transfer post-synthesis process, using hexadecyl trimethyl ammonium bromide (CTAB, cetyl trimethyl ammonium bromide) as transfer agent. This larger synthetic procedure assures the advantage of the organic phase method (small and monodisperse nanoparticles) and the aqueous medium required for the preparation of the gel material. Fig. 6 shows representative HRTEM of the as-prepared gel. This gel containing **3** and magnetite nanoparticles exhibits exactly the same photochemical cyclability as that previously commented for gels containing azocompound **3** (Fig. 7 shows a set of optical spectra recorded for this gel together with cyclability data), while simultaneously presenting magnetic properties.

As the particles size decreases, a large percentage of all the atoms in a nanoparticle are surface atoms, which implies that surface and interface effects become more important. The two most studied finite-size effects in nanoparticles are the single-domain limit and the superparamagnetic limit [27]. It is well known that spherical nanoparticles of magnetite form single-domain even for a diameter of 128 nm and depending of this size the temperature limit for the superparamagnetic behavior (blocking temperature, T_B) changes [15d]. So, magnetite nanoparticles smaller than 20 nm are usually superparamagnetic at room temperature, it means that the magnetic moment of the nanoparticles fluctuates in response to thermal energy, overcoming the anisotropy energy (E_A) and there is no coercive field (H_C). However, upon cooling, this superparamagnetic behavior turns into typical field dependence, showing H_C.

On the other hand, one of the greatest influences on the magnetic behavior of nanoparticles may be exercised by the magnetic interactions, the higher interactions the bigger coercive field. Additionally, the Stoner–Wolhfarth theory for single-domain particles predicts that the H_C of the nanosized materials depends also on the anisotropy constant (K). Organic ligands used to stabilize the magnetic nanoparticles have an influence on their magnetic properties, that is, ligands can modify the anisotropy of the metal atoms located at the surface of the particles [28]. In consequence, when the surfaces of the nanoparticles are modified or adsorb different molecules, the anisotropy constant changes, leading to changes in the H_C.

The magnetic properties of the gel were measured before and after irradiation of the sample (at room temperature in a photoreactor at 350 nm) at 2 K, below the T_B. Therefore non-zero coercive field was expected, because as mentioned above, the normal superparamagnetic behavior of magnetite nanoparticle have been canceled, due to the spin blockage, as a result of the low temperature. Figs. 8 and 9 show the hysteresis loops obtained in both cases. Note that the measurements were not performed under irradiation but after irradiating the sample. As can be seen in Fig. 9 the hysteresis loop obtained after irradiation shows a slightly higher coercive field (ca. 2.5 mT = 25 G) but no change in the saturation magnetization. Since between both measurements the sample is heated to room temperature and kept at room temperature during the irradiation process, in order to discard any interference due to the temperature variation, we have also performed blank measurements repeating the heating of the sample but without any irradiation. These measurements (Fig. 8) show no change at all between both hysteresis cycles, within experimental error, demonstrating that the changes observed in the hysteresis loops cannot be attributed to any thermal effect but to the irradiation itself. Since the differences in the hysteresis loop are only observed after irradiation of the sample, we can conclude that these reproducible changes in the hystere-

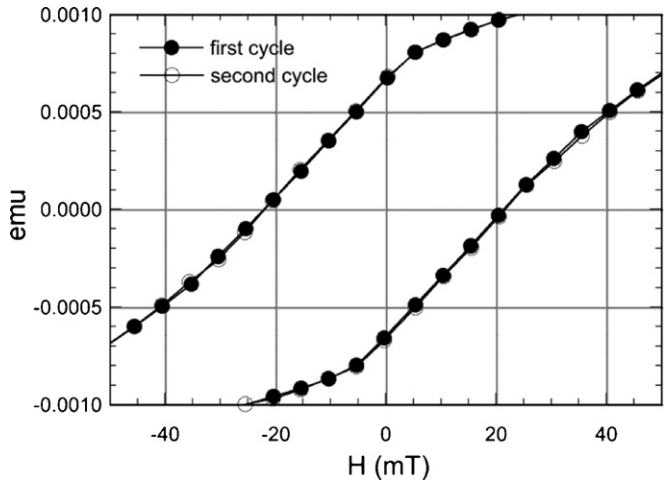

Fig. 8. Hysteresis loops at 2 K of the gel prepared with **3** before and after heating the sample to room temperature and without irradiation.

sis loop are due to the *trans–cis* isomerization of the azocompound **3**. As mentioned above, the hysteresis loops of magnetic materials are very sensitive to the distance between the nanoparticles due to their interaction and the changes in the coordination shell around the magnetic center since the spin dynamics of the magnetic nanoparticles is strongly dependent on their size and environment [29–31] and, therefore, it is proposed that those molecules of **3** that are coordinated to the iron oxide nanoparticles and undergoing the *trans–cis* isomerization are responsible for inducing slight changes in the distance between the nanoparticles and/or nanoparticle environment and, consequently in the coercive field of the hysteresis cycle.

These changes indicate that the original oleic acid/CTAB capping around the nanoparticle has been partially exchanged by azocompound **3** through the carboxylate groups analogous to those of oleic acid and, thus, some azocompound **3** molecules are acting as a new capping agent. Then, upon irradiation of the azocompound **3**, occurrence of the *trans–cis* isomerization of the azocompound and variation of the hysteresis loop of the iron oxide nanoparticles, takes place. Apparently magnetite nanoparticles containing trans azocompound **3** have somewhat different magnetic properties than those magnetite nanoparticles coordinated to the *cis* isomer. In addition, other possibility would be that the changes in the dimensions of the *trans* and *cis* isomers makes the interactions between the magnetic nanoparticles vary as consequence of the distance between them.

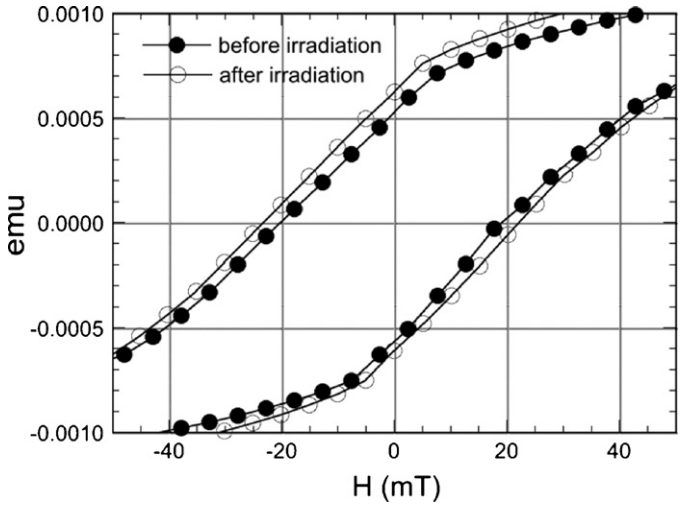

Fig. 9. Hysteresis loops at 2 K of the gel prepared with **3** before and after UV irradiation.

3. Experimental

All reagents were of commercial grade and were used as received without further purification. Methyl Orange (4-[[(4-dimethylamino)phenyl]-azo]benzenesulfonic acid sodium salt), iron tris(acetylacetonate) ($Fe[acac]_3$), 1,2-hexadecanediol, oleic acid, oleylamine, were obtained from Aldrich. 4-Hydroxyazobenzene-4′-sulfonic acid and azobenzene-4,4′-dicarboxylic acid were obtained from TCI. Phenyl ether, ammonium hydroxide, ethanol, hexane and dichloromethane were obtained from Scharlau and silicon dioxide Aerosil (a fumed silica constituted by nanoparticles of uniform size below 20 nm) was obtained from Degussa. The synthesis of the materials and the visible-light photoisomerization experiments were carried out with Milli-Q water.

3.1. Preparation of azocompound solutions

Samples were prepared by dissolving the compounds **1**–**3** in Milli-Q water, reaching a concentration 10^{-5} M. In the particular case of compound **3**, it was necessary to add a base to dissolve the sample correctly. For this purpose we employed 2 M sodium hydroxide.

3.2. Preparation of photoresponsive gels

The azobenzene-containing gels were synthesized by mixing an aqueous solution of **1**–**3** (10^{-4} M), previously alkalinized with sodium hydroxide (2 M) until the sample was completely dissolved (final pH = 11, yellowish solution), in the case of azocompound **3**. Then 5 g of Aerosil were added to the initial solution (100 mL) and the mixture was vigorously stirred during 5 min. Finally the sample was placed on a preheated oven at 70 °C for 3 h to generate a yellowish dense and viscous gel that does not fall down upon turning the vial upside down.

3.3. Synthesis of Fe_3O_4 nanoparticles

The synthesis of Fe_3O_4 was carried out following the high temperature organic-phase method described by Sun and Zeng [26]. According to this method, a mixture of iron tris(acetylacetonate) ($Fe[acac]_3$, 2 mmol), 1,2-hexadecanediol (10 mmol), oleic acid (6 mmol) and oleylamine (6 mmol) was dissolved in phenyl ether (20 mL), under argon and refluxed for 30 min. The mixture was cooled to room temperature and the nanoparticles precipitated after the addition of 80 mL of ethanol. The dark-brown solid was recovered by centrifugation and dissolved in hexane (20 mL) in the presence of 5 μL of oleic acid and 5 μL of oleylamine. The washing process was repeated twice without the addition of oleic acid and oleylamine and finally the solid nanoparticles were suspended in chloroform (60 mL).

The transfer of the Fe_3O_4 nanoparticles to the aqueous phase was performed using a modification of the method developed by Fan et al. [32]. An aqueous solution of CTAB (0.1 M, 30 mL) was added to the chloroform solution of the nanoparticles (15 mL), forming a two-phase system. The chloroform was removed in a rotavapor, resulting in a homogeneous brown aqueous solution of Fe_3O_4 nanoparticles.

3.4. Preparation of the photoresponsive magnetic gels

The incorporation of magnetite into photoresponsive gels was performed by mixing 5 mL of the aqueous iron oxide nanoparti-

cles suspension with 100 mL of a solution of azobenzene **3** (10^{-4} M, pH = 11), resulting in a color change of the solution from yellowish to brown. The so-obtained mixture clearly exhibited the Tyndall effect when irradiated with a laser beam. Then, 5 g of Aerosil were added to the azocompound/nanoparticle suspension and the resulting mixture was vigorously stirred during 5 min, finally the sample was placed on a preheated oven at 70 °C for 3 h, and a brownish thick gel was obtained (~5% of iron respect to Si determined by electron probe microanalysis, EPMA).

3.5. Photoisomerization experiments

A Luzchem photoreactor equipped with 10 tunable quasi-monochromatic mercury lamps emitting between 300 nm and 355 nm were used for most of the *trans–cis* reactions, including those performed on the gel for the magnetic measurements. For *cis–trans* isomerization a visible light projector equipped with a 200 W mercury lamp was used. The temperature of the sample was always lower than 35 °C by means a digital temperature controller.

3.6. Instrumental techniques

All UV–vis spectra were conducted using a Varian Cary-5G UV–vis spectrophotometer. The samples were measured in 10 mm light path Hellma quartz precision cells in the case of azobenzene solutions and in a 1 mm light path Hellma quartz precision cell in the case of gel. Spectra of all the samples were measured in transmission mode against air in the reference path. Laser flash photolysis experiments were carried out in a Luzchem ns laser flash system using the third (355 nm) harmonic of a Q-switched Nd:YAG laser for excitation (pulse $\leq$ 10 ns) and a 175 W ceramic Xenon Fiberoptic Lightsource, Cermax, perpendicular to the laser beam, as a probing light. The signal from the monochromator/photomultiplier detection system was captured by a Tektronix TDS 3032B digitizer. Laser system and digitizer are connected to a PC computer via GPIB and serial interfaces that controlled all the experimental parameters and provided suitable processing and data storage capabilities. The software package has been developed in the LabVIEW environment from National Instruments and compiled as a stand-alone application. The samples contained on Suprasil quartz $0.7 \times 0.7\ cm^2$ cuvettes capped with septa were purged with a N_2 or O_2 flow for at least 15 min before laser experiments. Metallic atomic composition of bulk samples was determined by means of EPMA analysis performed in a Philips SEM-XL30 equipped with an EDAX microprobe. HRTEM studies of photoresponsive magnetic gels were carried out on a JEM-2010 microscope (JEOL, Japan) operating at 200 kV. Samples were deposited on a carbon-coated copper grid and were tested when they were dried. The digital analysis of the HRTEM micrographs was done using DigitalMicrographTM 1.80.70 for GMS 1.8.0 by Gatan. Magnetic measurements were carried out with a Quantum Design (SQUID) Magnetometer MPMS-XL-5. The susceptibility data were corrected for the diamagnetic contributions calculated using the Pascal constants. The magnetization studies were performed between −5 and +5 T at 2 K. The sample was placed on a transparent sealed plastic bag that had been previously measured in the same conditions. In a first run the hysteresis cycle of the magnetization of the sample was measured at 2 K and then the sample was heated at room temperature and allowed to stand at room temperature during several minutes. After this heating, the sample was again cooled to 2 K and the hysteresis cycle measurement was repeated without noticing any difference between both cycles. In a second run we performed a first hysteresis cycle at 2 K. Then the sample was heated and irradiated at room temperature during ca. 15 min in a UV reactor. After irradiation, the sample was immediately placed into liquid nitrogen, inserted in the SQUID magnetometer at 100 K and cooled to 2 K in less than 30 min and the hysteresis cycle was repeated. Note that in order to remove any possible influence of the thermal history on the magnetic behavior of the samples, we have performed exactly the same thermal treatment to all the samples. Furthermore, the reproducibility of the measurements was checked for up to three different samples that gave very similar results.

4. Conclusions

In the present work we have shown that azobenzene-4,4′-dicarboxylic acid (**3**) is a suitable derivative that exhibits reversible *trans-cis* isomerization triggered by irradiation of the most stable *trans* isomer in aqueous solutions. Other azobenzenes having sulfonic acid groups do not undergo photoinduced trans/cis isomerization in water at the natural pH arising from the solution of the compounds (pH values: 8.7 and 6.3 for azobenzenes **1** and **2**, respectively) as evidenced by fast spectroscopic techniques with nanosecond resolution. Compound **3** shows photoresponse with a high photochemical reversibility. We have taken advantage of the reversible *trans* to *cis* isomerization of azobenzene **3** even in gel, and its ability to bind a Fe_3O_4 nanoparticles to prepare for the first time a soft matter in which the hysteresis loop is influenced by light through the photoisomerization event. We propose that the photoisomerization alters the distance between the nanoparticles or the coordination sphere of the same and these changes are reflected in the coercitive field of the iron oxide nanoparticles. Our studies will be expanded in the future towards the preparation of photo-responsive materials having stronger coupling between their magnetic properties and photo-isomerization.

Acknowledgements

This work has been supported by the EU (MolSpinQIP and the ERC SPINMOL Advanced Grant), the Spanish Ministerio de Ciencia e Innovación with FEDER cofinancing (Project Consolider-Ingenio in Molecular Nanoscience CSD2007-00010 and projects MAT2007-61584, CTQ2009-11583 and CTQ-2008-06720) and the Generalitat Valenciana (PROMETEO program). The authors thank Maykel de Miguel his kindly assistance with the laser flash photolysis experiments.

References

[1] H. Rau, in: Z. Sekkat, W. Knoll (Eds.), Photoreactive Organic Thin Films, Academic Press, Amsterdam, 2002, pp. 3–47.
[2] A. Gilbert, J. Baggott, Essentials of Organic Photochemisry, Blackwell, Oxford, 1990.
[3] G.S. Kumar, D.C. Neckers, Chem. Rev. 89 (1989) 1915–1925.
[4] J. Griffiths, Chem. Soc. Rev. 1 (1972) 481–493.
[5] K. Ichimura, Chem. Rev. 100 (2000) 1847–1873.
[6] M. Alvaro, M. Benitez, D. Das, H. Garcia, E. Peris, Chem. Mater. 17 (2005) 4958–4964.
[7] A.S. Kumar, T. Ye, T. Takami, B.-C. Yu, A.K. Flatt, J.M. Tour, P.S. Weiss, Nano Lett. 8 (2008) 1644–1648.
[8] V. Ferri, M. Elbing, G. Pace, M.D. Dickey, M. Zharnikov, P. Samori, M. Mayor, M.A. Rampi, Angew. Chem., Int. Ed. 47 (2008) 3455–3457.
[9] G. Pace, V. Ferri, G. Grave, M. Elbing, C. Hänisch, M. Zharnikov, M. Mayor, M.A. Rampi, P. Samorì, Proc. Natl. Acad. Sci. U.S.A. 104 (2007) 9937–9942.
[10] J. Zeitouny, C. Aurisicchio, D. Bonifazi, R. De Zorzi, S. Geremia, M. Bonini, C.-A. Palma, P. Samorì, A. Listorti, A. Belbakrab, N. Armaroli, J. Mater. Chem. 19 (2009) 4715–4724.
[11] N. Henningsen, K.J. Franke, G. Schulze, I. Fernández-Torrente, B. Priewisch, K. Rück-Braun, J.I. Pascual, ChemPhysChem 9 (2008) 71–73.
[12] M. Han, D. Ishikawa, T. Honda, E. Itob, M. Hara, Chem. Commun. 46 (2010) 3598–3600.
[13] M.J. Comstock, N. Levy, A. Kirakosian, J. Cho, F. Lauterwasser, J.H. Harvey, D.A. Strubbe, J.M.J. Frechet, D. Trauner, S.G. Louie, M.F. Crommie, Phys. Rev. Lett. 99 (2007) 038301.
[14] K.G. Yager, C.J. Barrett, J. Photochem. Photobiol. A 182 (2006) 250–261.
[15] (a) B.L. Cushing, V.L. Kolesnichenko, J. O'Connor, Chem. Rev. 104 (2004) 3893–3946;

(b) Y. Jun, J. Choi, J. Cheon, Angew. Chem. Int. Ed. 45 (2006) 3414–3439;
(c) J. Park, J. Joo, S.G. Kwon, Y. Jang, T. Hyeon, Angew. Chem. Int. Ed. 46 (2007) 4630–4660;
(d) A. Lu, E.L. Salabas, F. Schüth, Angew. Chem. Int. Ed. 46 (2007) 1222–1244;
(e) S.G. Kwon, T. Hyeon, Acc. Chem. Res. 41 (12) (2008) 1696–1709;
(f) S. Laurent, D. Forge, M. Port, A. Roch, C. Robic, L.V. Elst, R.N. Muller, Chem. Rev. 108 (2008) 2064–2110.
[16] (a) R. Gangopadhyay, A. De, Chem. Mater. 12 (2000) 608–622;
(b) K. Hervé, L. Douziech-Eyrolles, E. Munnier, S. Cohen-Jonathan, M. Soucé, H. Marchais, P. Limelette, F. Warmont, M.L. Saboungi, P. Dubois, I. Chourpa, Nanotechnology 19 (2008) 465–608;
(c) L. Wang, J. Sun, J. Mat. Chem. 18 (2008) 4042–4049;
(d) C. Tu, Y. Yang, M. Gao, Nanotechnology 19 (2008) 105601;
(e) S. Li, j. Qin, A. Fornara, M. Toprak, M. Muhammed, D.K. Kim, Nanotechnology 20 (2009) 185607;
(f) J. Li, L. Guo, L. Zhang, C. Yu, L. Yu, P. Jiang, C. Wei, F. Qin, J. Shi, Dalton Trans. (2009) 823–831.
[17] (a) S. Nie, S.R. Emory, Science 275 (1997) 1102–1106;
(b) R.G. Ispasoiu, L. Balogh, O.P. Varnavski, D.A. Tomalia, T. Goodson III, J. Am. Chem. Soc. 122 (2000) 11005–11006;
(c) W.U. Huynh, J.J. Dittmer, A.P. Alivisatos, Science 295 (2002) 2425–2427;
(d) A.H. Yuwono, J. Xue, J. Wang, H.I. Elim, W. Ji, Y. Li, T.J. White, J. Mat. Chem. 13 (2003) 1475–1479.
[18] (a) J.D. MacKenzie, E.P. Bescher, Acc. Chem. Res. 40 (9) (2007) 810–818;
(b) M. Niederberger, Acc. Chem. Res. 40 (9) (2007) 793–800.
[19] N.J. Dunn, W.H. Humphries, A.R. Offenbacher, T.L. King, J.A. Gray, J. Phys. Chem. A 113 (47) (2009) 13144–13151.
[20] A. Dirksen, E. Zuidema, R.M. Williams, L. De Cola, C. Kauffmann, F. Vögtle, A. Roque, F. Pina, Macromolecules 25 (2002) 2743–2747.
[21] A.M. Sanchez, M. Barra, R.H. de Rossi, J. Org. Chem. 64 (1999) 1604–1609.
[22] W. Freyer, D. Brete, R. Carley, R. Schmidt, C. Gahl, M. Weinelt, J. Photochem. Photobiol. A 204 (2009) 102–109.
[23] T. Ikeda, M. Nakano, Y. Yu, O. Tsutsumi, A. Kanazawa, Adv. Mater. 15 (2003) 201–205.
[24] Y.-L. Zhao, J.F. Stoddart, Langmuir 25 (15) (2009) 8442–8446.
[25] A. Pich, S. Bhattacharya, Y. Lu, V. Boyko, H.-J.P. Adler, Langmuir 20 (24) (2004) 10706–10711.
[26] S. Sun, H. Zeng, J. Am. Chem. Soc. 124 (2002) 8204–8205.
[27] (a) D. Peddis, C. Cannas, A. Musinu, G. Piccaluga, Chem. Eur. J. 15 (2009) 7822–7829;
(b) Y.W. Jun, J.W. Seo, J. Cheon, Acc. Chem. Res. 41 (2) (2008) 179–189.
[28] P.M. Paulus, H. Bönnemann, A.M. van der Kraan, F. Luis, J. Sinzig, L.J. de Jongh, Eur. Phys. J. D 9 (1999) 501–504.
[29] K. Takeda, K. Agawa, Phys. Rev. B 54 (1997) 14560.
[30] M. Clemente-León, H. Soyer, E. Coronado, C. Mingotaud, C.J. Gómez-García, P. Delhaès, Angew. Chem. 37 (1998) 2842–2845.
[31] M. Wei, K. Okabe, H. Arakawa, Y. Teraoka, New J. Chem. 26 (2002) 20–23.
[32] H. Fan, K. Yang, D.M. Boyle, T. Sigmon, K.J. Malloy, H. Xu, G.P. López, C.J. Brinker, Science 304 (2004) 567–571.